Zero-valent iron addition in anaerobic dynamic membrane bioreactors for preconcentrated wastewater treatment: Performance and impact

Yisong Hu[a,c,*], Ying Zang[a], Yuan Yang[a], Ao Duan[a], Xiaochang C. Wang[a,b], Huu Hao Ngo[b,d], Yu-You Li[c], Runda Du[c]

[a] Key Lab of Northwest Water Resource, Environment and Ecology, MOE, Xi'an University of Architecture and Technology, Xi'an 710055, P.R. China

[b] International Science & Technology Cooperation Center for Urban Alternative Water Resources Development, Xi'an 710055, P.R. China

[c] Department of Civil and Environmental Engineering, Graduate School of Environmental Studies, Tohoku University, 6-6-06 Aza-Aoba, Aramaki, Aoba-ku, Sendai, Miyagi 980-8579, Japan

[d] Centre for Technology in Water and Wastewater, School of Civil and Environmental Engineering, University of Technology Sydney, Sydney, NSW 2007, Australia

* Corresponding author: Y. Hu (Tel.: +8602982205652; E-mail: huyisong@xauat.edu.cn)

Abstract: Wastewater preconcentration to capture abundant organics is promising for facilitating subsequent anaerobic digestion (AD) to recover bioenergy, however research efforts are still needed to verify the effectiveness of such an emerging strategy as carbon capture plus AD. Therefore, lab-scale anaerobic dynamic membrane bioreactors (AnDMBRs) without and with the addition of zero-valent iron (ZVI) (i.e., AnDMBR1 versus AnDMBR2) were developed for

preconcentrated domestic wastewater (PDW) treatment, and the impact of ZVI addition on process performance and associated mechanisms were investigated. The stepwise addition of ZVI from 2 to 4 to 6 g/L improved the treatment performance as COD removal slightly increased and TP removal and methane production were enhanced by 53.3%-62.9% and 22.6%-31.3%, respectively, in consecutive operational phases. However, the average increasing rate of the transmembrane pressure (TMP) in AnDMBR2 (0.18 kPa/d) was obviously higher than that in AnDMBR1 (0.05 kPa/d), indicating an unfavorable impact of dosing ZVI on the dynamic membrane (DM) filtration performance. ZVI that has transformed to iron ions (mainly Fe^{2+}) can behave as a coagulant, electron donor or inorganic foulant, thus enabling the excellent removal of dissolved phosphorous, enhancing the enrichment and activities of specific methanogens and causing the formation of a compact DM layer. Morphological, componential, and microbial community analyses provided new insights into the functional mechanisms of ZVI added to membrane-assisted anaerobic digesters, indicating that ZVI has the potential to improve bioenergy production and resource recovery, while optimizing the ZVI dosage should be considered to alleviate membrane fouling.

Keywords: anaerobic dynamic membrane bioreactor; zero-valent iron; preconcentrated wastewater; carbon capture; bioenergy recovery; biochemical methane production

1. Introduction

Anaerobic digestion is highly applicable for treating organic-rich waste streams, such as industrial wastewater (Dereli et al., 2012), sewage sludge (Zhen et al., 2017), food wastes (Nghiem et al., 2017), and landfill leachate (Renou et al., 2008). Successful applications of AD for low-strength wastewater (like domestic wastewater) are noted in tropical areas (notably in Latin America and India) (Lettinga et al., 2001; Chernicharo, et al., 2015), but rarely reported in temperate or cold regions due to low water temperatures and low organic strengths (McKeown, et al., 2012). Moreover, the extra costs of heating a large amount of domestic wastewater to high temperatures make the AD process not economically feasible.

An innovative concept of "carbon capture" that can enrich sufficient organic matters from the wastewater is highly attractive (Wang et al., 2018; Alloul et al., 2018). Several measures can achieve wastewater preconcentration for organics enrichment, such as chemical enhanced sedimentation, high-loaded membrane bioreactors, and membrane filtration (Ansari et al., 2016; Jin et al., 2017; Xiong et al., 2019; Hube et al., 2020). However, in the preconcentrated wastewater substantial suspended solids are retained in the meantime, which will affect subsequent AD process for efficient bioenergy recovery (Chong et al., 2012; Zhang et al., 2018). Although, the biochemical methane production (BMP) can be as high as 0.2-0.25 L CH_4/gVSS·d (Gao et al., 2019; Xiong et al., 2019), while in large anaerobic digesters the performance reduction may occur due to varied operational parameters.

Recently, zero-valent iron (ZVI), a reductive material, has been extensively used in-situ for enhancing the AD of wastewater and solid wastes, with methane yields increased by 10.1%-159% depending on the substrates adopted and the type and dosage of ZVI (Liu et al., 2012; Feng et al., 2014; Zhang et al., 2014; Hao et al., 2017; Wei et al., 2018). The mechanisms supposed for ZVI in promoting the AD process are listed as follows: (1) ZVI addition can create a more favorable AD environment by reducing the oxidation-reduction potential (Zhen et al., 2015; Liu et al., 2011) and possibly changing the fermentation type (Ren et al., 2001; Ren et al., 2007); (2) ZVI stimulates the rate of hydrolysis/acidogenesis by improving the activity of related microbial enzymes (Feng et al., 2014; Wei et al., 2018); (3) ZVI might preferentially enrich specific methanogens such as hydrotrophic methanogens to maintain the balance between H_2 production and consumption (Feng et al., 2014); and (4) ZVI can serve as an electron donor (Wei et al., 2018; Zhen et al., 2015) and a conductive material to promote electron transfer (Hao et al., 2017). However, these mechanisms are still ambiguous and may play the roles synthetically; thus, more efforts are needed to clarify their accurate contributions to the AD process (Zhao et al., 2018). The application of ZVI in preconcentrated wastewater treatment is of great interest. Moreover, most of the studies regarding the ZVI-based AD process have been limited to batch tests or lab-scale experiments using conventional anaerobic digesters, and little attention has been paid to membrane-assisted anaerobic processes (such as anaerobic membrane bioreactors) (Hu et al., 2018a). In this circumstance, iron in different forms (Fe^0, Fe^{2+} and Fe^{3+}) may affect membrane filterability as flux

enhancers or potential inorganic foulants (Meng et al., 2017); however, to date, little is known about this issue.

Therefore, in this study the major objective is to investigate the impact of ZVI on preconcentrated domestic wastewater (PDW) treatment in the emerging AnDMBR process during long-term continuous operation, mainly focusing on the system performance, sludge properties and functional mechanisms involved. Analytical techniques were used to characterize the properties of the bulk sludge and dynamic membrane (DM) layer in the AnDMBRs, which included excitation-emission matrix (EEM) fluorescence spectroscopy, particle size distribution analysis, scanning electron microscopy (SEM), energy-diffusive X-ray (EDX) analysis, and high-throughput pyrosequencing. The results will provide a better understanding of the functional mechanism and practical application of ZVI in the membrane-based AD process.

2. Materials and methods

2.1. Experimental setup and operation

Two AnDMBRs with an effective working volume of 3.5 L were established and operated with preconcentrated domestic wastewater as the influent, and the schematic diagram of the AnDMBRs is shown in Fig. 1. AnDMBR1 without ZVI addition was used as the control reactor, while in AnDMBR2, ZVI was added with the dosage increasing from 2 to 4 and 6 g/L with the suitable ZVI dosage according to our previous batch experiments (Zang et al., 2020). Each upflow AnDMBR contained one

submerged DM module. The flat-sheet DM module is homemade with 75 μm nylon mesh as the supporting material and a total filtration area of 0.02 m^2 for both sides. Two peristaltic pumps (Longer BT-100, China) were used for wastewater feeding and effluent extraction in one bioreactor. To detect the DM filtration behavior, an online pressure sensor (SIN-P400, China) was employed to automatically record the transmembrane pressure (TMP). There is neither biogas scouring nor mixed liquor recycling in AnDMBRs, thus the up-flow velocity (approximately 0.7 m/h) was caused by influent feeding.

Fig. 1.

The biogas yield was recorded by a wet-type gas flowmeter (TC-2, China), and the methane content in the biogas was detected by daily sampling and measurement. A constant flux (5.5 L/m^2h) was maintained, resulting in an HRT of 32 h. The temperature in the bioreactors was controlled at approximately 37 ℃ by using a water bath device. Strictly anaerobic environment was maintained in the AnDMBRs since the dissolved oxygen (DO) was undetectable and the oxidation-reduction potential (ORP) was in the range of 300-350 mV.

The stable operational period of 85 days could be divided into three phases, namely Phase I, II and III, according to a stepwise increase in the ZVI dosage from 2 g/L to 4 and 6 g/L in the AnDMBR2. The durations of the three phases are 10 d, 60 d and 15 d. There was no other difference in the operational conditions during the three sequential phases, and one DM module in each bioreactor was continuously used during the entire operation period without replacement due to sustainable filtration performance.

2.2. Preconcentrated domestic wastewater, inoculum and ZVI

The experiment was conducted at a local domestic wastewater treatment plant (WWTP). Wastewater was collected from this WWTP and then subjected to a dynamic membrane filtration (DMF) process to obtain the preconcentrated wastewater, and the details regarding the DMF process for PDW production can be found in our previous work (Xiong et al., 2019). The quality of preconcentrated domestic wastewater is presented in Table 1, and the sulfate content is 70.3±10.5 mg/L based on several measurements.

Table 1

The inoculum for the AnDMBRs was from a full-scale anaerobic digester. The sludge was gravity thickened and inoculated into two bioreactors with an initial mixed liquor suspended solids (MLSS) concentration of 10935 mg/L, a mixed liquor volatile suspended solids (MLVSS) content of 5362 mg/L and a MLVSS/MLVSS ratio of 49%. No sludge was discharged except for sampling for sludge properties analysis.

Zero valent iron (purity >99%) with a mean diameter of 0.15 mm was obtained from Aladdin Corp. (Shanghai, China). ZVI particles were stored in a sealed bottle filled with pure nitrogen gas.

2.3. Analytical methods

2.3.1. Sample collection and pretreatment

To characterize its various properties, part of the DM layer on the mesh surface was collected by using a plastic sheet from the AnDMBRs at the end of the operational period. The DM sludge was further subjected to dilution with pure water and gentle

mixing (Hu et al., 2018b), and the total suspended solids (TSS) and volatile suspended solids (VSS) were measured subsequently. The TSS and VSS contents in the DM layer can be calculated according to the TSS and VSS concentrations collected from a certain membrane area. Moreover, the DM layer was also sampled and dried naturally for SEM-EDX analysis. Extracellular polymeric substances (EPS), including soluble type (SEPS) and bound type (BEPS), were extracted from the sludge samples with the heat treatment method (Hu et al., 2016).

2.3.2. Analysis of common parameters

Common indexes, such as the chemical oxygen demand (COD), total phosphorus (TP), PO_4^{3-}, TN, ammonia (NH_3-N), sulfate, sludge concentration, total iron and ferrous ion (Fe^{2+}) were measured frequently (Chinese NEPA, 2002). Turbidity was measured with a 2100N turbidity meter (Hach, USA), while the ORP was detected by a portable meter (Hatch, USA). The biogas composition (such as CH_4, CO_2, N_2, and H_2) was measured by a gas chromatograph (Tianmei, China) (Hu et al., 2018b), while the volatile fatty acids (VFAs) were analyzed with a liquid chromatograph (LC-10AD, Shimadzu, Japan) (Tang et al., 2017).

The main components of the EPS, namely proteins and polysaccharides, were detected using chemical analytical methods. Proteins and polysaccharides were analyzed according to the modified Lowry method (Hartree, 1972) and the Anthrone-sulfuric acid method (Loewus, 2002).

The statistical analyses were accomplished by using IBM SPSS Statistics 20.0 software (International Business Machines Co., USA) based on reported method

(Yang et al., 2020). In detail, the differences in COD removal and specific methanogenic activities in the two AnDMBRs were determined using one-way analysis of variance (ANOVA), and the significant difference level was assessed based on the P value obtained ($P< 0.05$ indicating a significant difference).

2.3.3. Analytical techniques

To detect the morphology and chemical elements of the anaerobic sludge, DM layer and nylon mesh, SEM (VEGA 3LMH, Tescan Corporation, Czech) and an EDX analyzer (Oxford INCA Energy 350, UK) were applied. The X-ray diffraction patterns (XRD) of the potential Fe-based precipitates in the sludge samples were measured based on a Rigaku Ultimate IV diffractometer at room temperature (CuKα radiation, 10–80°) (Yang et al., 2019).

The 3D-EEM fluorescence spectra of the dissolved organic matters (DOM) in the influent, sludge supernatant and effluent as well as EPS samples were measured by a fluorescence spectrofluorometer (F-7000, Hitachi, Japan). The excitation wavelengths were from 220 nm to 450 nm, with the emission ranging from 220 nm to 550 nm. The stepwise increase in the excitation wavelength and excitation wavelength were the same as 5 nm.

To better understand the microbial community structure, the high-throughput pyrosequencing method was used based on previous studies (Hu et al., 2017; Quek, et al., 2017; Yang et al., 2020). Before high-throughput 16S rRNA gene pyrosequencing, DNA extraction and PCR amplification were firstly performed.

2.3.4. Analysis of specific methanogenic activities

The specific methanogenic activities (SMA) of sludge samples from the AnDMBRs were tested in duplicate with 120 mL serum bottles (Chen et al., 2017; Yang et al., 2020). The substrates used included preconcentrated domestic wastewater (2 g/L, 50 mL), sodium acetate (2 g/L, 50 mL) and H_2/CO_2 (V/V=2:8, 1.4 atm). The seed sludge for the batch tests (20 mL) was acquired from the bioreactors at the end of the operational time, with an MLVSS concentration of 8-9 g/L, resulting in the food/microorganism (F/M) ratios of 0.5-0.7 gCOD/gMLVSS. 10 mL of the nutrient solution was supplemented with the recipe according to the literature (Yang et al., 2020). The tests were conducted on a shaking table (120 rpm) at 35 °C. After frequently measuring the biogas yield and composition for several days, the SMAs were determined by linear fitting or simulating the modified Gompertz equation as Eq. (1) (Chen et al., 2017).

$$P = P_0 \cdot \exp\left\{-\exp\left[\frac{R_{max} \times e}{P_0}(\lambda - t) + 1\right]\right\} \quad (1)$$

where P is the cumulative methane production ($mLCH_4/gVSS$), P_0 is the maximum potential of methane production ($mLCH_4/gVSS$), R_{max} (or SMA) is the maximum methane production rate ($mLCH_4/gVSS \cdot d$), $e = 2.7183$, λ is the lag time (day), and t is the cultivation time (day).

3. Results and discussion

3.1. Process performance

3.1.1. Filtration behavior

Fig. 2 presents the variations of the TMP and effluent turbidity with the filtration time. In this study, the constant flux operation mode was applied at a filtration flux of 5.5 L/m^2h, and thus, the changes in the TMP can be used to roughly reflect the DM filtration behavior. During phase I (0-10 d), a slight TMP increase was noted for the AnDMBR1 and AnDMBR2, and the average TMP increasing rates (dTMP/dt) were 0.4 and 0.5 kPa/d. However, in Phase II (11-70 d), a fast increase of TMP followed by a gradual increase was noted in AnDMBR2 with ZVI addition, whereas a low TMP increasing rate of 0.03 kPa/d was found for the control reactor (AnDMBR1). At the end of this period, the TMP of the AnDMBR2 was approximately 20 kPa, which was much higher than that (8 kPa) in the AnDMBR1. For Phase III, although the ZVI concentration was enhanced to 6 g/L in the AnDMBR2, a relatively stable TMP was maintained at 20 kPa, while AnDMBR1 still showed low TMP values ranging from 5 to 7 kPa. The results indicated the adverse effect of ZVI addition on the DM filtration behavior, especially at higher ZVI dosages (4-6 g/L).

Fig. 2.

The influent turbidity ranged from 588.0 to 1036.8 NTU during the long-term operation period, while in the first day, the permeate turbidity of both AnDMBRs was as high as 40-100 NTU, as shown in Fig. 2, indicating the ineffective retention of fine particles during the initial DM formation stage. Thereafter, the effluent turbidity decreased to below 20 NTU and remained relatively stable approximately 20 NTU in the AnDMBRs. No obvious changes in the effluent turbidity were observed until the end of the operation time. The slightly higher permeate turbidity values in the

AnDMBR2 indicated the potential effect of ZVI. Overall, the turbidity removal rates were above 95% in the two AnDMBRs. The turbidity removal performance was similar to previous reports for other AnDMBRs but worse than that of aerobic DMBRs with a stable effluent turbidity as low as less than 5 NTU (Chu et al., 2014; Hu et al., 2016), which is likely due to differences in the influent quality, operational conditions and sludge properties.

3.1.2. Pollutant removal and methane production

Table 2 shows the removal of some pollutants of concern, including COD, TN, TP NH_3 and PO_4^{3-}. Apparently, ZVI addition had little effect on the COD removal, as the removal rates were above 97% in the AnDMBR2, while a similar COD removal performance was also noted in the AnDMBR1. However, the effluent COD concentration was slightly lower (8-15 mg/L) in the AnDMBR2 compared to the control bioreactor, with a significant difference noted ($P<0.05$). No removal of TN and NH_3 was observed due to the inhibition of nitrogen conversion in a strictly anaerobic environment. As for TP and PO_4^{3-}, AnDMBR2 showed high removal rates of over 95%, while much lower removal efficiencies were found in AnDMBR1 (especially for PO_4^{3-}), indicating that adding ZVI largely enhanced PO_4^{3-} removal possibly by chemical precipitation rather than biological means (refer to Section 3.3 for a detailed discussion).

Table 2

Methane production in the AnDMBRs using preconcentrated domestic wastewater as substrates can be found in Table 2. Generally, methane generation was lower than

those (approximately 0.2 L CH_4/gCOD·d) reported in batch biomethane production potential (BMP) tests using similar wastewater (Xiong et al., 2019), indicating the important effects of operational conditions and the reactor scale on methane production. As shown in Table 1, the preconcentrated domestic wastewater had much lower SCOD/COD ratios (9.7%-18.3%) and higher TS contents (1.5-1.6 g/L) compared to raw domestic wastewater, indicating the abundance of substantial particulate organics that adversely affected methane production and also the necessity to further characterize and pre-treat PDW to achieve better bioenergy recovery. However, some differences were noted between the two AnDMBRs regarding the methane yield. Firstly, the methane contents in the produced biogas ranged from 70% to 78%, while higher methane proportion was always noted in the AnDMBR2 compared to AnDMBR1. Enhanced methane contents in biogas with ZVI addition were also reported by previous studies (Feng et al., 2014; Wei et al., 2018), which presumed that during the AD process ZVI causing H_2 evolution enhanced the generation of acetate by syntrophic acetogenic bacteria and the reduction of CO_2 and H_2 to methane by serving as an electron donor. During the entire operational period, AnDMBR1 showed relatively stable methane yields of 0.044-0.049 L CH_4/gCOD·d, while the methane yield increasing from 0.043 to 0.061 and 0.065 L CH_4/gCOD·d were noted in AnDMBR2 with a stepwise ZVI dosage. In comparison with AnDMBR1, in Phase III, the methane yield in AnDMBR2 was enhanced by 31.3%. Various mechanisms by which ZVI improves anaerobic digestion have been proposed, such as ZVI corrosion and hydrogen evolution (Dinh et al., 2004), enhancing

hydrolysis-acidification process (Zang et al., 2020), serving as an essential element and potential electron donor (Wei et al., 2019), and conducting direct metal-microbe electron transfer (Tang et al., 2019), with most concerns being discussed later.

As an effective filter consisting of microorganisms and various organic and inorganic substances derived from bulk sludge, the DM layer was also responsible for the removal of dissolved organics (such as volatile fatty acids and soluble COD) in addition to solid-liquid separation (i.e., rejection of suspended solids). To reveal the potential retention effect of the formed DM layers in the AnDMBRs, the SCOD and fluorescent DOM from influent, sludge supernatant and effluent samples during Phase III were analyzed. The experimental results showed that the DM layer contributed to 4.8%-7.7% of SCOD removal based on the COD concentration differences between the sludge supernatant and the permeate to the influent COD in both AnDMBRs. Similar phenomena regarding the retention of SCOD or VFAs by the cake layer in AnMBRs and AnDMBRs have been reported in previous studies (Ersahin, et al., 2016; Smith, et al., 2013). Moreover, one study reported substantial biogas production in the cross-flow DM module in an AnDMBR accompanied with SCOD reduction across the DM layer, further proving the existence and contribution of active biomass in the DM layer (Alibardi, et al., 2016).

Fluorescent DOMs belonging to high to medium molecular weight substances were noted to cause irreversible membrane fouling (such as pore blocking) in aerobic and anaerobic MBRs (Dereli, et al., 2012; Meng, et al., 2017), possibly resulting in a reduction in the porosity of the DM layer. Thus, the possible retention of such DOMs

is worthy of attention. EEM spectra of fluorescent DOM samples during Phase III are shown in Fig. 3. Three fluorescence peaks were observed in the DOM samples, peak A (310–325 nm/405–415 nm) representing humic-acid-like substances, peak B (280 nm/335–345 nm) reflecting tryptophan-protein-like substances, and peak C (225–240 nm/305–345 nm) indicating aromatic-protein-like substances (Chen et al., 2003).

By comparing the fluorescence parameters, such as the peak location and fluorescence intensity (FI), it was noted that abundant protein-like substances (peak B and peak C) existed in the influent, the FI of the two peaks largely decreased in the sludge supernatant, and a further decrease in the FI was observed in the effluent in both AnDMBRs. The results indicated that protein-like substances with the properties of readily biodegradation and high molecular weight could be more easily removed in the AnDMBRs through biodegradation and DM layer retention. However, due to their lower molecular weight and biodegradability (Li et al., 2019; Yang et al., 2020), humic-acid-like substances (peak A) showed lower FI values in all the samples independent of ZVI addition, indicating their weak retention by the DM layer and their low impacts on DM fouling. A careful comparison showed that AnDMBR2 presented better removal of all types of fluorescent DOMs (especially protein-like substances), which was consistent with higher biogas yields by the conversion of organics and more severe membrane fouling resulting from the retention and accumulation of various foulants during long-term operation.

Fig. 3.

3.2. Properties of bulk sludge and DM layers

3.2.1. Morphological and component analysis

Fig. 4 presents the morphology and elementary composition of the bulk sludge and DM layer from both AnDMBRs. From Fig. 4 (a)-(d), the bulk sludge samples seemed to be different from the DM layers. The bulk sludge was more porous and rougher in structure, consisting of diverse components with different sizes and shapes, while the DM layer was gel-like and less porous (especially in AnDMBR2). Moreover, the bulk sludge sample in AnDMBR2 was denser, possibly due to the modification of sludge properties (such as the structure and density) by ZVI. Under an anaerobic environment, ZVI can be converted to iron ions, which will function as a coagulant to promote the aggregation of fine particles, colloids and biopolymers through various coagulation mechanisms (such as charge neutralization), depending on the iron ion concentration and sludge properties (Meng et al., 2007).

Fig. 4.

As shown in Fig. 4 (e)-(h), the major elements, including C, O, P, S, Fe, Al, Mg, Ca, Cu, Si, Na, K and Cl, were detected in the bulk sludge and DM layers using the EDX analyzer. Comparing the bulk sludge from the two AnDMBRs, it was observed that the dominant elements in AnDMBR1 were C (41.5%) and O (35.9%), the contents of which decreased to 21.7% and 23.1%, respectively, in the AnDMBR2. The most concerned elements (including P, S and Fe) accounted for 5.1%, 1.2% and 1.7%, respectively, in AnDMBR1 and 7.5%, 2.3% and 43.6% in AnDMBR2. The interactions among these elements (such as P, S, and Fe) in AnDMBR2 with the addition of ZVI likely contributed to the increase in their contents. As for the

elemental distribution in the DM layers, the contents of C, O, P, S, and Fe in the DM layer from AnDMBR1 were 53.2%, 24.4%, 3.5%, 1.9% and 1.1%, respectively, and 60.6%, 23.7%, 4.2%, 2.2% and 5.6%, respectively, in AnDMBR2, indicating the potential interactions across Fe, C, P and S to simultaneously enhance their contents. In addition, based on the XRD patterns of the bulk sludge and cake layer from the two AnDMBRs (Fig. S1. in Supporting Information), it is verified that the Fe-P and Fe-S precipitates in the AnDMBR2 are more abundant than those in the AnDMBR1, in the forms of ferrous phosphate ($Fe_3(PO_4)_2$), ferric phosphate (FePO4), iron sulfide (FeS), and others. Thus, the results indicated that adding ZVI to membrane-based anaerobic digesters could affect the components and structure of both the bulk sludge and fouling layer.

3.2.2. Microbial community analysis

Fig. 5(a) shows the classification of bacteria at the class level and their relative abundance in various sludge samples, including inoculation sludge, bulk sludge and the DM layers. Regardless of the sludge samples, the most predominant bacterial class were *Deltaproteobacteria*, *Betaproteobacteria*, *Gammaproteobacteria*, *Alphaproteobacteria*, *Anaerolineae*, *Clostridia*, *Flavobacteriia*, *Bacteroidia*, *Synergistia*, *Planctomycetia*, *Methanomicrobia* and *Caldisericia*, which belonged to the phyla of *Proteobacteria*, *Chloroflexi*, *Firmicutes*, *Bacteroidetes*, *Synergistete*, *Planctomycetes*, *Euryarchaeota*, *Parcubacteria* and *Caldiserica*. Most of the detected phyla were responsible for the degradation of organics to achieve hydrolysis-acidification and acetogenesis (Gao et al., 2010; Quek, et al., 2017). The

selective enrichment of *Chloroflexi*, *Firmicutes*, *Acidobacteria* and the reduction of *Proteobacteria* in the AnDMBR2 indicated the effects of ZVI addition on the evolution of functional bacteria. Special attention is paid to the phylum *Proteobacteria* as *the* genus *Smithella* (propionate-degrading bacteria), *Syntrophobacter and Syntrophorhabdus* (syntrophic bacteria), *Geobacter* (electro-active bacteria), *Desulfomicrobium and Desulfoprunum* (sulfate-reducing bacteria) are responsible for different microbial metabolic activities (Wang et al., 2020). Except the decrease in the abundance of the genus *Smithella*, other genus above mentioned are all enriched with ZVI addition in the AnDMBR2 compared with the AnDMBR1. Additionally, it has been reported that *Bacteriodetes* can potentially contribute to fouling and biofilm formation through the release of proteinaceous EPS (Gao et al., 2010), showing a higher relative abundance (7.5%) in the DM layer from the AnDMBR2 rather than that (4.13%) from the AnDMBR1. Several phyla, such as *Synergistetes*, *Verrucomicrobia*, *Parcubacteria* and *Caldiserica*, were also detected in the two AnDMBRs, although with lower relative abundances.

However, it was interesting to note that the aforementioned phyla showed a higher relative abundance in the DM layer compared to the bulk sludge, likely due to their stronger resistance to extreme environmental conditions (less available substrates and living space in the DM layers). The phylum *Ignavibacteriae*, which is reported to be related to sulfur utilization, was only found in AnDMBR2 (in both the bulk sludge and the DM layer), possibly because the formed Fe-S based compounds with ZVI addition might be utilized by *Ignavibacteriae*.

Fig. 5.

Fig. 5(b) depicts the relative abundance of the archaea communities at the genus level in the aforementioned sludge samples. The predominant genera in all the sludge samples were *Methanothrix*, *Methanobacterium*, *Methanolinea*, *Methanospirillum*, *Methanoregula*, *Methanosphaerula*, *Methanomassiliicoccus*, and *Methanomethylovorans*, followed by the others. *Methanothrix* and *Methanomethylovorans* (in the same order of *Methanosarcinales*) belongs to acetoclastic methanogens that can use acetate and methyl compounds as the carbon source, while the others are hydrogenotrophic methanogens (some genera simultaneously use formate as an organic substrate) (Demirel and Scherer, 2008). It was obvious that the relative abundance of *Methanothrix* and *Methanolinea* increased, while that of *Methanobacterium* and *Methanospirillum* decreased in the bulk sludge from the AnDMBR2 compared to the AnDMBR1. The enrichment of *Methanothrix* (acetoclastic methanogen) and *Methanolinea* (hydrogenotrophic methanogen) in the bulk sludge from the AnMBR2 might be due to H_2 production with ZVI addition, which simulated the growth of hydrogen-consuming microorganisms (homoacetogens and hydrogenotrophic methanogens) (Feng et al., 2014). A recent study showed the evidence that *Geobacter* and *Methanothrix* species cooperated via direct interspecies electron transfer (DIET), and *Geobacter* species could provide electrons to *Methanothrix* species for methane production by the reduction of carbon dioxide (Holmes et al., 2017). The syntrophic metabolism among *Geobacter* and *Methanothrix* species can be promoted by ZVI addition as an electron donor and

conductive material, which is reasonable as enhanced methane generation, higher methane content in the biogas and more enrichment of *Geobacter* species are all noted in the AnDMBR2 compared with the AnDMBR1. As for the DM layer, some differences were noted (especially for AnDMBR2) because a reduction in the relative abundance of *Methanothrix* accompanied by the increase in *Methanolinea* and *Methanospirillum* was observed. The enrichment of hydrogenotrophic methanogens rather than acetoclastic methanogens was likely due to a lack of access to more preferred substrate (acetic acid) in the DM layer. It is also observed that some genera, such as *Methanothrix*, *Methanospirillum* and *Metanomethylovorans*, can use sulfide as a sulfur source during their proliferation, thus possibly contributing to the conversion and removal of sulfide in anaerobic digesters.

3.3. Impacts of ZVI addition on membrane-based AD system

3.3.1. P removal

In this work, a moderate removal of TP (32%-42%) and no removal of PO_4^{3-} were noted in AnDMBR1, while AnDMBR2 demonstrated excellent removal (95%-97%) of both TP and PO_4^{3-} during the entire operational period. Therefore, more attention was paid to the effect of adding ZVI on phosphorous removal. The most important mechanism was supposed to be the formation of precipitates by interactions of PO_4^{3-} and iron ion. It has been reported that the added ZVI in an anaerobic digester could be converted to iron ions (mainly Fe^{2+}) accelerated by specific microorganisms (such as sulfate-reducing bacteria, homoacetogens and hydrogenetrophic methanogens) and release electrons to function as an electron donor to promote H_2 production (Dinh et

al., 2004; Lai et al., 2012; Zhen et al., 2015), or CO_2 reduction to CH_4 (Rotaru et al., 2014) as shown in Eqs. (2)- (4), or even direct metal-microbe electron transfer (Tang et al., 2019). From Eq. (5), it is supposed that PO_4^{3-} can be removed by forming precipitates, such as $Fe_3(PO_4)_2{\cdot}8H_2O$. It was reported that $Fe_3(PO_4)_2{\cdot}8H_2O$, also called vivianite, was commonly found in digested sludge, accounting for the majority of the Fe-P bound compounds (Fang et al., 2018; Wu et al., 2019); thus, phosphorus recovery via vivianite formation has received a substantial amount of scientific attention (Fang et al., 2020; Liu et al., 2020).

Furthermore, by comparing the contents of Fe^{2+} and total iron in the influent, sludge supernatant and effluent, as illustrated in Table 3, it was noted that although the total iron and Fe^{2+} in the influent were always lower than 1 mg/L, the iron ion contents in the sludge supernatant and effluent were obviously different in AnDMBR1 and AnDMBR2. In all the samples from AnDMBR1, the total iron ions and Fe^{2+} were 1 mg/L or lower. However, in AnDMBR2, with the improvement of the ZVI dosage, the total iron in the sludge supernatant increased from 19.8 to 21.7 and 28.1 mg/L accompanied by a relatively stable Fe^{2+} content ranging from 17.6 to 21.8 mg/L. As for the effluent, a great reduction in the total iron content to 4.7-6.5 mg/L and a reduction in the Fe^{2+} content to 0.5-1.0 mg/L were noted. The results indicated several important findings: 1) excess Fe^{2+} existed in the sludge supernatant even after Fe^{2+} consumption by potential reactions among Fe^{2+} and PO_4^{3-}, S^{2-}, biopolymers, and others; and 2) a high retention of Fe^{2+} by the DM layer (95%-98%) in AnDMBR2 was observed.

$Fe^0 \rightarrow Fe^{2+} + 2e^-$ (2)

$2H^+ + 2e^- \rightarrow H_2$ (3)

$CO_2 + 8e^- + 8H^+ \rightarrow CH_4 + 2H_2O$ (4)

$2PO_4^{3-} + 3Fe^{2+} + 8H_2O \rightarrow Fe_3(PO_4)_2 \cdot 8H_2O \downarrow$ (5)

$SO_4^{2-} \rightarrow S^{2-}$ (6)

$Fe^{2+} + S^{2-} \rightarrow FeS \downarrow$ (7)

As shown in Eqs. (6)-(7), other inorganic and organic substances, such as SO_4^{2-}/S^{2-} and biopolymers, might contribute to the decrease of the total iron and Fe^{2+} in the AnDMBR2. The interaction of Fe^{2+} and S^{2-} to form FeS precipitate might contribute to the reduction of Fe^{2+}, as documented previously (Lai et al., 2012). Although S^{2-} may compete with PO_4^{3-} to form Fe-coupled precipitates when Fe^{2+} is limited in wastewater, this condition did not seem to exist in this study due to the higher Fe^{2+} concentration in the sludge supernatant. It is deduced that PO_4^3 and sulfide will be almost completely removed by forming chemical precipitates, which was also verified by the EDX analysis in Section 3.2.1. Moreover, abundant Fe^{2+} from ZVI conversion likely enhanced the capture of biopolymers, fine particle and some solutes, thus contributing to the removal of pollutants and the modification of sludge properties.

Table 3

3.3.2. Membrane fouling issue

A distinct difference in the DM filtration behavior of the two AnDMBRs indicated that ZVI addition had a negative impact on DM permeability, at least within the dosage range applied in this work. Table 4 presents the major properties of the DM layer

collected at the end of Phase III. It was found that the DM layer in AnDMBR2 was much thicker due to the accumulation of more total solids (TS), volatile solids (VS) and organic matter (polysaccharides and proteins) compared to that in AnDMBR1. It was considered that during the initial DM formation stage, the DM layers in the AnDMBRs were almost the same in structure and filtration ability. However, with the stepwise ZVI addition in the AnDMBR2, ZVI will gradually modify the properties of the bulk sludge by releasing iron ions to work as a coagulant. However, the effect of iron ions on sludge properties can be positive or negative depending on the dosage (Meng et al., 2007). As discussed, the sludge properties (such as the particle size and flocculating ability) became worse at higher ZVI dosages, possibly due to the over dosage of ZVI to release excess Fe^{2+} that adversely affects biomass physicochemical properties.

Table 4

In addition, a large amount of total iron and Fe^{2+} in the sludge supernatant would eventually contact the DM layer, and the retention rates of total iron and Fe^{2+} by the DM layer in the AnDMBR2 were 67.3%-81.2% and 95.3%-97.4%, respectively. This contributed to the inorganic fouling through the interactions between the iron ions and the attached substances (such as fine flocs and biopolymers), which would be enhanced by the continuous release of iron ions with stepwise ZVI addition. As a result, both organic and inorganic fouling were more serious in AnDMBR2, as shown by the compact DM layer with less pores and a lower roughness, resulting in much higher TMP values and total filtration resistances.

3.3.3. Specific methanogenic activities

ZVI addition into the anaerobic digesters will change the bulk sludge properties from various aspects (such as the floc structure and filtration ability). More importantly, it can alter the microbial properties of the bulk sludge, including the microbial community (as mentioned previously) and the microbial metabolism activities discussed herein. Fig. 6 shows the results of SMA tests of bulk sludge samples from two AnDMBRs, using preconcentrated WW, sodium acetate and the mixture of H_2/CO_2 (80%: 20%) as the substrates. From Fig. 6(a), it was supposed that during long-term operation, the anaerobic sludge in both bioreactors was acclimatized to the substrate conditions of PDW, and thus, no lag time for methane production was noted during the SMA tests. Based on methane production data of the first 24 h, the SMA of anaerobic sludge was calculated to be 58.8 and 63.3 mL CH_4/gMLVSS·d for AnDMBR1 and AnDMBR2, respectively, statistically different ($P<0.05$). As shown in Fig. 6 (b) and (c), when considering the two main pathways for methanogenesis, the SMA for acetoclastic methanogenesis was 182.9 and 150.0 mL CH_4/gMLVSS·d, respectively ($P<0.05$), while the SMA for hydrogenotrophic methanogenesis was 37.5 and 59.0 mL CH_4/gMLVSS·d, respectively, for the two AnDMBRs ($P>0.05$). The SMA tests indicated that ZVI addition enhanced hydrogenotrophic methanogenesis by 57% while substantially inhibiting the acetoclastic methanogenesis process by 18.0% (likely due to substrate limitation as only acetate was supplied as an available substrate), thus eventually enhancing the overall methane production activity when PDW was adopted as the substrate.

Fig. 6.

The results were in agreement with the relative abundance of various methanogens and the methane production performance in the bioreactors. The enhanced multiplication of hydrogen-consuming methanogens, including homoacetogens and hydrogenotrophic methanogens, in anaerobic digesters after ZVI addition has also been documented in other studies (Feng et al., 2014; Zhao et al., 2018). It was supposed that ZVI firstly contributed to H_2 production and a favorable anaerobic environment (lower oxidation-reduction potential) (Ren et al., 2001; Wei et al., 2018), which subsequently promoted the enrichment of hydrogen-consuming methanogens with correspondingly enhanced methanogenic activities.

3.4. Implication of ZVI addition for practical applications

The ZVI was supplemented into a membrane-based anaerobic digestion system (i.e., the AnDMBR process) to study the potential effects and associated mechanisms. The experimental results showed that AnDMBR alone could be stably operated for PDW treatment for a long time without any physical or chemical cleaning, while ZVI addition further enhanced pollutant removal (COD, P and S) and bioenergy generation and modified the sludge characteristics but negatively affected the DM filtration behavior. While the overall fouling rate of AnDMBR2 is 0.18 kPa/d is acceptable as it is still much lower than those noted in some AnMBRs (around 1 kPa/d) (Wang et al., 2018), indicating the superior filterability of DM enabling minimum membrane maintenance in practical applications. As for the mechanisms of methane production

enhancement, ZVI corrosion and hydrogen evolution can be evidenced by continuous Fe^{2+} releasing and the enrichment of hydrogen-consuming anaerobic microbes, especially hydrogenotrophic methanogens. Since the PDW containing a large portion of particulate COD, the enhanced hydrolysis-acidification process will also contribute to more methane production according to our batch tests (Zang et al., 2020). Recently it is suggested that with the coexistence of anaerobic microbes ZVI can take part in the direct metal-microbe electron transfer, inducing the direct reduction of CO_2 to CH_4 as a novel methane production pathway (Tang et al., 2019), but still requiring further verification. Indeed, ZVI addition can improve methane production during the AD process, however it is associated with such complex biochemical interactions that deserves more academic attention in the future.

In addition, the extra cost of ZVI supplementation and the fouling issue might reduce the attraction and competitiveness of the developed process. However, the commercial ZVI can be replaced by the low-cost wasted iron scraps, thus further reducing the chemical cost, as previously investigated (Zhen et al., 2015; Wei et al., 2018). With a careful attention to ZVI dosage, the extra cost of ZVI addition and inorganic membrane fouling can be reasonably controlled. In this work, ZVI added into the bioreactor based on one-time addition can play the role for a long time (i.e. more than one month), actually resulting in a daily dosage of less than 70 mg. Economic evaluation of iron-based AD has shown that the expenditure caused by ZVI addition (including transportation and dosing) can be completely offset by the enhanced CH_4 production (Wei et al., 2018; Zang et al., 2020). Moreover, there

remains substantial space to enhance AD performance by combining ZVI and other pretreatment methods (Zhen et al., 2017) to establish more effective strategies for PDW treatment.

To date, the current work mainly aimed to develop and verify the ZVI-enhanced AnDMBR process for preconcentrated domestic wastewater treatment, following the sustainable principle of achieving the maximal recovery of various resources (such as water, bioenergy and value-add chemicals). However, further optimization of the established system is still necessary, with the main concerns being the utilization of low-cost ZVI, the control of suitable ZVI dosages to avoid detrimental effects and the development of combined pretreatment strategies to enhance the anaerobic digestion efficiency (especially for the hydrolysis-acidification process). If these aspects are fully taken into consideration from the techno-economic point of view, the practical application of ZVI-based AnDMBR treatment can be expected.

4. Conclusions

The impacts of ZVI on anaerobic digestion of the PDW were investigated in continuously operated AnDMBRs. In AnDMBR2, with a stepwise increase in the ZVI dosage, the COD removal was not affected while methane production was enhanced by 31.3% in Phase III. TP and PO_4^{3-} were significantly removed, likely due to chemical precipitation (P-Fe interaction). ZVI addition showed an adverse effect on DM filterability indicated by the higher TMP increasing rate. Continuous Fe^{2+} releasing contributed to the change of sludge properties, and the structure and

filterability of the DM layer. Adding ZVI promoted hydrogenotrophic methanogenesis activity rather than acetoclastic methanogenesis activity, however substantial enrichment of H_2-utilizing and acetate-utilizing methanogens was observed. The ZVI-based AnDMBR process can be promising for bioenergy production and resource recovery if the suitable ZVI dosage and process optimization are further considered.

Acknowledgements

This study was supported by the Natural Science Foundation of Shaanxi Province (grant no. 2018JQ5054), the Japan Society for the Promotion of Science (JSPS) support for JSPS Fellows (no. P19745), the Science Foundation for Fostering Talents of Xi'an University of Architecture and Technology (No. RC1710), and the Shaanxi Provincial Program for Innovative Research Team (grant nos. 2019TD-025 and IRT2013KCT-13).

References

[1] Alibardi, L., Bernava, N., Cossu, R., Spagni, A., 2016. Anaerobic dynamic membrane bioreactor for wastewater treatment at ambient temperature. Chem. Eng. J. 284, 130–138.

[2] Alloul, A., Ganigué, R., Spiller, M., Meerburg, F., Cagnetta, C., Rabaey, K., Vlaeminck, S.E., 2018. Capture–Ferment–Upgrade: A Three-Step Approach for the Valorization of Sewage Organics as Commodities. Environ. Sci. Technol. 52, 6729–6742.

[3] Ansari, A.J., Hai, F.I., Guo, W., Ngo, H.H., Price, W.E., Nghiem, L.D., 2016. Factors governing the pre-concentration of wastewater using forward osmosis for subsequent resource recovery. Sci. Total Environ. 566–567, 559-566.

[4] Chen, R., Nie, Y., Kato, H., Wu, J., Utashiro, T., Lu, J., Yue, S., Jiang, H., Zhang, L., Li, Y.-Y., 2017. Methanogenic degradation of toilet-paper cellulose upon sewage treatment in an anaerobic membrane bioreactor at room temperature. Bioresour. Technol. 228, 69–76.

[5] Chen, W., Westerhoff, P., Leenheer, J.A., Booksh, K., 2003. Fluorescence Excitation−Emission Matrix Regional Integration to Quantify Spectra for Dissolved Organic Matter. Environ. Sci. Technol. 37, 5701–5710.

[6] Chernicharo, C.A.L., van Lier, J.B., Noyola, A., Ribeiro, T.B., 2015. Anaerobic sewage treatment: state of the art, constraints and challenges. Rev. Environ. Sci. Biotechnol. 14, 649–679.

[7] Chinese NEPA, Water and Wastewater Monitoring Methods, 4th ed., Chinese Environmental Science Publishing House, Beijing, China, 2002.

[8] Chong, S., Sen, T.K., Kayaalp, A., Ang, H.M., 2012. The performance enhancements of upflow anaerobic sludge blanket (UASB) reactors for domestic sludge treatment: A State-of-the-art review. Water Res. 46, 3434–3470.

[9] Chu, H., Zhang, Y., Zhou, X., Zhao, Y., Dong, B., Zhang, H., 2014. Dynamic membrane bioreactor for wastewater treatment: Operation, critical flux, and dynamic membrane structure. J. Membr. Sci. 450, 265–271.

[10] Demirel, B., Scherer, P., 2008. The roles of acetotrophic and hydrogenotrophic methanogens during anaerobic conversion of biomass to methane: a review. Rev. Environ. Sci. Bio. 7, 173–190.

[11] Dereli, R.K., Ersahin, M.E., Ozgun, H., Ozturk, I., Jeison, D., van der Zee, F., van Lier, J.B., 2012. Potentials of anaerobic membrane bioreactors to overcome treatment limitations induced by industrial wastewaters. Bioresour. Technol. 122, 160–170.

[12] Dinh, H. T., Kuever, J., Mußmann, M., Hassel, A. W., Stratmann, M., Widdel, F., 2004. Iron corrosion by novel anaerobic microorganisms. Nature, 427, 829-832.

[13] Ersahin, M.E., Gimenez, J.B., Ozgun, H., Tao, Y., Spanjers, H., van Lier, J.B., 2016. Gas-lift anaerobic dynamic membrane bioreactors for high strength synthetic wastewater treatment: Effect of biogas sparging velocity and HRT on treatment performance. Chem. Eng. J. 305, 46–53.

[14] Fang, L., Liu, R., Li, J., Xu, C., Huang, L. Z., Wang, D., 2018. Magnetite/Lanthanum

hydroxide for phosphate sequestration and recovery from lake and the attenuation effects of sediment particles. Water Res. 130, 243-254

[15] Fang, L., Zeng, W., Xu, L., Huang, L. Z., 2020. Green rusts as a new solution to sequester and stabilize phosphate in sediments under anoxic conditions and their implication for eutrophication control. Chem. Eng. J. 388, 124198.

[16] Feng, Y., Zhang, Y., Quan, X., Chen, S., 2014. Enhanced anaerobic digestion of waste activated sludge digestion by the addition of zero valent iron. Water Res. 52, 242–250.

[17] Gao, D.-W., Zhang, T., Tang, C.-Y., Wu, W.-M., Wong, C.-Y., Lee, Y.H., Yeh, D.H., Criddle, C.S., 2010. Membrane fouling in an anaerobic membrane bioreactor: differences in relative abundance of bacterial species in the membrane foulant layer and in suspension. J. Membr. Sci. 364, 331–338.

[18] Gao, Y., Fang, Z., Liang, P., Zhang, X., Qiu, Y., Kimura, K., Huang, X., 2019. Anaerobic digestion performance of concentrated municipal sewage by forward osmosis membrane: Focus on the impact of salt and ammonia nitrogen. Bioresour. Technol. 276, 204–210.

[19] Hao, X., Wei, J., Van Loosdrecht, M.C.M., Cao, D., 2017. Analysing the mechanisms of sludge digestion enhanced by iron. Water Res. 117, 58–67.

[20] Hartree, E.F.,1972. Determination of protein: a modification of the Lowry method that gives linear photometric response. Anal. Biochem. 48, 422–427.

[21] Holmes, D.E., Shrestha, P.M., Walker, D.J., Dang, Y., Nevin, K.P., Woodard, T.L., Lovley, D.R., 2017. Metatranscriptomic evidence for direct interspecies electron transfer between Geobacter and Methanothrix species in methanogenic rice paddy soils. Appl. Environ. Microbiol. 83, e00223-17.

[22] Hu, Y., Wang, X.C., Tian, W., Ngo, H.H., Chen, R., 2016. Towards stable operation of a dynamic membrane bioreactor (DMBR): Operational process, behavior and retention effect of dynamic membrane. J. Membr. Sci. 498, 20–29.

[23] Hu, Y., Yang, Y., Wang, X.C., Ngo, H.H., Sun, Q., Li, S., Tang, J., Yu, Z., 2017. Effects of powdered activated carbon addition on filtration performance and dynamic membrane layer properties in a hybrid DMBR process. Chem. Eng. J. 327, 39–50.

[24] Hu, Y., Wang, X.C., Ngo, H.H., Sun, Q., Yang, Y., 2018a. Anaerobic dynamic membrane bioreactor (AnDMBR) for wastewater treatment: A review. Bioresour. Technol. 247,

1107–1118.

[25] Hu, Y., Yang, Y., Yu, S., Wang, X.C., Tang, J., 2018b. Psychrophilic anaerobic dynamic membrane bioreactor for domestic wastewater treatment: effects of organic loading and sludge recycling. Bioresour. Technol. 270, 62–69.

[26] Hube, S., Eskafi, M., Hrafnkelsdóttir, K.F., Bjarnadóttir, B., Bjarnadóttir, M.Á., Axelsdóttir, S., Wu, B., 2020. Direct membrane filtration for wastewater treatment and resource recovery: A review. Sci. Total Environ. 710, 136375.

[27] Jin, Z., Meng, F., Gong, H., Wang, C., Wang, K., 2017. Improved low carbon-consuming fouling control in long-term membrane based sewage pre-concentration: the role of enhanced coagulation process and air backflushing in sustainable sewage treatment. J. Membr. Sci. 529, 252–262.

[28] Lai, B., Zhou, Y., Yang, P., 2012. Passivation of Sponge Iron and GAC in Fe0/GAC Mixed-Potential Corrosion Reactor. Ind. Eng. Chem. Res. 51, 7777–7785.

[29] Lettinga, G., Rebac, S., Zeeman, G., 2001. Challenge of psychrophilic anaerobic wastewater treatment. Trends Biotechnol. 19, 363–370.

[30] Li, K., Wen, G., Li, S., Chang, H., Shao, S., Huang, T., Li, G., Liang, H., 2019. Effect of pre-oxidation on low pressure membrane (LPM) for water and wastewater treatment: A review. Chemosphere 231, 287–300.

[31] Liu, K., Li, F., Cui, J., Yang, S., Fang, L., 2020. Simultaneous removal of Cd (II) and As (III) by graphene-like biochar-supported zero-valent iron from irrigation waters under aerobic conditions: Synergistic effects and mechanisms. J. Hazard. Mater. 395, 122623.

[32] Liu, Y., Zhang, Y., Quan, X., Chen, S., Zhao, H., 2011. Applying an electric field in a built-in zero valent iron - Anaerobic reactor for enhancement of sludge granulation. Water Res. 45, 1258–1266.

[33] Liu, Y., Zhang, Y., Quan, X., Li, Y., Zhao, Z., Meng, X., Chen, S., 2012. Optimization of anaerobic acidogenesis by adding Fe^0 powder to enhance anaerobic wastewater treatment. Chem. Eng. J. 192, 179–185.

[34] Loewus, F.A., 2002. Improvement in Anthrone Method for Determination of Carbohydrates. Anal. Chem. 24, 219.

[35] Meng, F., Zhang, H., Yang, F., Liu, L., 2007. Characterization of cake layer in submerged

membrane bioreactor. Environ. Sci. Technol. 41, 4065–4070.

[36] Meng, F., Zhang, S., Oh, Y., Zhou, Z., Shin, H.-S., Chae, S.-R., 2017. Fouling in membrane bioreactors: An updated review. Water Res. 114, 151–180.

[37] McKeown, R.M., Hughes, D., Collins, G., Mahony, T., O'Flaherty, V., 2012. Low temperature anaerobic digestion for wastewater treatment. Curr. Opin. Biotech. 23, 444–451.

[38] Nghiem, L.D., Koch, K., Bolzonella, D., Drewes, J.E., 2017. Full scale co-digestion of wastewater sludge and food waste: Bottlenecks and possibilities. Renew. Sust. Energ. Rev. 72, 354–362.

[39] Quek, P.J., Yeap, T.S., Ng, H.Y., 2017. Applicability of upflow anaerobic sludge blanket and dynamic membrane-coupled process for the treatment of municipal wastewater. Appl. Microbiol. Biotechnol. 101, 6531–6540.

[40] Renou, S., Givaudan, J.G., Poulain, S., Dirassouyan, F., Moulin, P., 2008. Landfill leachate treatment: Review and opportunity. J. Hazard. Mater. 150, 468–493.

[41] Ren, N., Chua, H., Chan, S., Tsang, Y., Wang, Y., Sin, N., 2007. Assessing optimal fermentation type for bio-hydrogen production in continuous-flow acidogenic reactors. Bioresour. Technol. 98, 1774–1780.

[42] Ren, N., Chen, X., Zhao, D., 2001. Control of fermentation types in continuous-flow acidogenic reactors: effects of pH and redox potential. J. Harbin. Inst. Technol. 8, 116–119.

[43] Rotaru, A. E., Shrestha, P. M., Liu, F., Shrestha, M., Shrestha, D., Embree, M., Zengler, K., Wardman, C., Nevina K.P., Lovley, D. R., 2014. A new model for electron flow during anaerobic digestion: direct interspecies electron transfer to Methanosaeta for the reduction of carbon dioxide to methane. Energ. Environ. Sci. 7, 408–415.

[44] Smith, A.L., Skerlos, S.J., Raskin, L., 2013. Pychrophilic anaerobic membrane bioreactor treatment of domestic wastewater. Water Res. 47, 1655–1665.

[45] Tang, H. Y., Holmes, D. E., Ueki, T., Palacios, P. A., Lovley, D. R., 2019. Iron corrosion via direct metal-microbe electron transfer. Mbio, 10(3), e00303-19.

[46] Tang, J., Wang, X.C., Hu, Y., Ngo, H.H., Li, Y., 2017. Dynamic membrane-assisted fermentation of food wastes for enhancing lactic acid production. Bioresour. Technol. 234, 40–47.

[47] Wang, G., Gao, X., Li, Q., Zhao, H., Liu, Y., Wang, X. C., Chen, R., 2020. Redox-based

electron exchange capacity of biowaste-derived biochar accelerates syntrophic phenol oxidation for methanogenesis via direct interspecies electron transfer. J. Hazard. Mater. 121726.

[48] Wang, K.M., Martin Garcia, N., Soares, A., Jefferson, B., McAdam E.J., 2018. Comparison of fouling between aerobic and anaerobic MBR treating municipal wastewater. H_2Open Journal, 1(2), 131–159.

[49] Wang, X., Daigger, G., Lee, D.-J., Liu, J., Ren, N.-Q., Qu, J., Liu, G., Butler, D., 2018. Evolving wastewater infrastructure paradigm to enhance harmony with nature. Sci. Adv. 4, eaaq0210.

[50] Wei, J., Hao, X., van Loosdrecht, M.C.M., Li, J.,2018. Feasibility analysis of anaerobic digestion of excess sludge enhanced by iron: A review. Renew. Sust. Energ. Rev. 89, 16–26.

[51] Wu, Y., Luo, J., Zhang, Q., Aleem, M., Fang, F., Xue, Z., Cao, J., 2019. Potentials and challenges of phosphorus recovery as vivianite from wastewater: A review. Chemosphere 226, 246–258.

[52] Xiong, J., Yu, S., Hu, Y., Yang, Y., Wang, X.C., 2019. Applying a dynamic membrane filtration (DMF) process for domestic wastewater preconcentration: organics recovery and bioenergy production potential analysis. Sci. Total Environ. 680, 35–43.

[53] Yang, S., Guo, X., Wang, Z., Dzakpasu, M., Dai, X., Ding, D., Wu, K., Huang, Y., Zhang, Q., Jin, P., Wang, X. C., 2019. Significance of B-site cobalt on bisphenol A degradation by MOFs-templated CoxFe3− xO4 catalysts and its severe attenuation by excessive cobalt-rich phase. Che. Eng. J. 359, 552-563.

[54] Yang, Y., Zang, Y., Hu, Y., Wang, X.C., Ngo, H.H., 2020. Upflow anaerobic dynamic membrane bioreactor (AnDMBR) for wastewater treatment at room temperature and short HRTs: Process characteristics and practical applicability. Chem. Eng. J. 383, 123186.

[55] Zang, Y., Yang, Y., Hu, Y., Ngo, H.H., Wang, X.C., Li, Y.-Y., 2020. Zero-valent iron enhanced anaerobic digestion of pre-concentrated domestic wastewater for bioenergy recovery: Characteristics and mechanisms. Bioresour. Technol. 310, 123441.

[56] Zhang, L., Vrieze, J.D., Hendrickx, T.L.G., Wei, W., Temmink, H., Rijnaarts, H., Zeeman, G., 2018. Anaerobic treatment of raw domestic wastewater in a UASB-digester at 10 ℃ and microbial community dynamics. Chem. Eng. J. 334, 2088–2097.

[57] Zhang, Y., Feng, Y., Yu, Q., Xu, Z., Quan, X., 2014. Enhanced high-solids anaerobic digestion of waste activated sludge by the addition of scrap iron. Bioresour. Technol. 159, 297–304.

[58] Zhao, Z., Zhang, Y., Li, Y., Quan, X., Zhao, Z., 2018. Comparing the mechanisms of ZVI and Fe_3O_4 for promoting waste-activated sludge digestion. Water Res. 144, 126–133.

[59] Zhen, G., Lu, X., Li, Y., Liu, Y., Zhao, Y., 2015. Influence of zero valent scrap iron (ZVSI) supply on methane production from waste activated sludge. Chem. Eng. J. 263, 461–70.

[60] Zhen, G., Lu, X., Kato, H., Zhao, Y., Li, Y.-Y., 2017. Overview of pretreatment strategies for enhancing sewage sludge disintegration and subsequent anaerobic digestion: Current advances, full-scale application and future perspectives. Renew. Sust. Energ. Rev. 69, 559–577.

Tables and Figure captions

Table 1 Quality of the preconcentrated domestic wastewater.

Table 2 Treatment performance of the AnDMBRs.

Table 3 Variations of total iron and Fe^{2+} in the liquid phase (unit: mg/L).

Table 4 Properties of anaerobic sludge and DM layer at the end of Phase III.

Fig. 1. Schematic diagram of the lab-scale AnDMBRs.

Fig. 2. Variations of TMP and effluent turbidity with operational time in the AnDMBRs.

Fig. 3. EEM spectra of fluorescent DOM samples from the AnDMBRs during Phase III.

Fig. 4. SEM-EDX analysis: (a) SEM photo of bulk sludge in AnDMBR1; (b) SEM photo of bulk sludge in AnDMBR2; (c) SEM photo of DM layer in AnDMBR1; (d) SEM photo of DM layer in AnDMBR2; (e) EDX profile of bulk sludge in AnDMBR1; (f) EDX profile of bulk sludge in AnDMBR2; (g) EDX profile of DM layer in AnDMBR1 and (h) EDX profile of DM layer in AnDMBR2.

Fig. 5. Microbial community analysis of sludge samples: (a) classification of bacterial communities at the class level and (b) classification of archaea communities at the genus level. (Inoculum means inoculum sludge; BS means bulk sludge; DM means dynamic membrane layer)

Fig. 6. SMA tests using different substrates: (a) preconcentrated domestic wastewater; (b) sodium acetate and (c) the mixture of hydrogen and carbon dioxide.

Table 1 Quality of the pre-concentrated domestic wastewater.

Item	Phase I	Phase II	Phase III
COD (mg/L)	2373±61	2066.06±459.23	2024.89±316.69
SCOD (mg/L)	433.9±46.17	225.23±50.96	195.53±30.76
SCOD/COD (%)	18.28	10.90	9.66
TN (mg/L)	57.58±7.35	47.33±21.02	61.57±3.78
TP (mg/L)	11.99±3.09	10.66±4.20	12.58±5.57
PO_4^{3-} (mg/L)	5.62±1.11	5.5±0.87	4.83±0.58
TS (g/L)	1.61±0.02	1.55±0.02	1.45±0.04
VS (g/L)	1.22±0.09	1.13±0.01	1.05±0.03
VS/SS (%)	75	73	72
pH	7.76±0.10	7.75±0.12	7.79±0.06

Table 2 Treatment performance of the AnDMBRs.

Item	Phase I		Phase II		Phase III	
	AnDMBR1	AnDMBR2	AnDMBR1	AnDMBR2	AnDMBR1	AnDMBR2
Effluent COD (mg/L)	57.18±1.31	42.65±1.17	56.79±6.27	46.71±7.34	57.23±3.21	49.06±4.08
Effluent SCOD (mg/L)	50.94±1.47	41.51±2.22	52.39±9.83	41.38±8.94	52.51±1.15	47.28±3.89
COD removal (%)	97.59	98.20	97.25	97.73	97.17	97.58
Effluent TN (mg/L)	-	-	48.36±18.2	53.44±6.60	40.57±1.79	40.95±9.51
Effluent NH_3 (mg/L)	-	-	45.8±9.88	44.1±4.21	46.97±8.37	39.93±2.68
Effluent TP (mg/L)	-	-	7.23±0.66	0.52±0.36	7.28±0.44	0.57±0.28
TP removal (%)	-	-	32.18	95.12	42.13	95.47
Effluent PO_4^{3-} (mg/L)	-	-	6.4±0.54	0.2±0.09	6.83±0.11	0.11±0.10
PO_4^{3-} removal (%)	-	-	-	96.36	-	97.72
Methane content (%)	73.59±3.98	76.23±5.50	75.77±2.30	77.86±3.61	69.85±6.53	72.55±5.38
Methane production (L/d)	0.27±0.02	0.27±0.04	0.26±0.04	0.32±0.03	0.26±0.03	0.34±0.03
Methane yield (LCH_4/gCOD·d)	0.044 ±0.003	0.044 ±0.007	0.049 ±0.008	0.060 ±0.006	0.049 ±0.006	0.065 ±0.006

Table 3 Variations of total iron and Fe^{2+} in the liquid phase (unit: mg/L).

Item	Phase I		Phase II		Phase III	
	AnDMBR1	AnDMBR2	AnDMBR1	AnDMBR2	AnDMBR1	AnDMBR2
Influent total iron	0.50±0.1		0.6±0.08		0.76±0.4	
Influent Fe^{2+}	0.36±0.07		0.47±0.1		0.38±0.05	
Sludge supernatant total iron	1.32±0.59	19.83±0.62	1.66±1.03	21.67±0.52	0.67±0.17	28.09±1.54
Sludge supernatant Fe^{2+}	0.48±0.06	17.6±0.47	0.62±0.09	17.7±2.06	0.37±0.03	21.83±1.33
Effluent total iron	0.86±0.68	6.48±0.17	0.97±0.71	4.67±2.25	0.44±0.07	5.29±0.88
Effluent Fe^{2+}	0.19±0.1	0.57±0.07	0.17±0.08	0.46±0.19	0.2±0.07	1.03±0.72

Table 4 Properties of anaerobic sludge and DM layer at the end of Phase III.

Item	AnDMBR1	AnDMBR2
Thickness of DM layer (mm)	1.01	1.36
TS of anaerobic sludge (g/L)	16.86±0.94	24.475±0.88
VS of anaerobic sludge (g/L)	8.36±0.36	9.385±0.47
VS/TS of anaerobic sludge (%)	0.495	0.383
TS of DM layer (g/m^2)	93.76±1.03	130.34±0.54
VS of DM layer (g/m^2)	36.58±0.52	55.25±0.54
VS/TS of DM layer (%)	39.01	42.39
Proteins in DM layer (g/m^2)	2.30±0.11	3.73±0.01
Polysaccharides in DM layer (g/m^2)	0.60±0.02	0.99±0.07

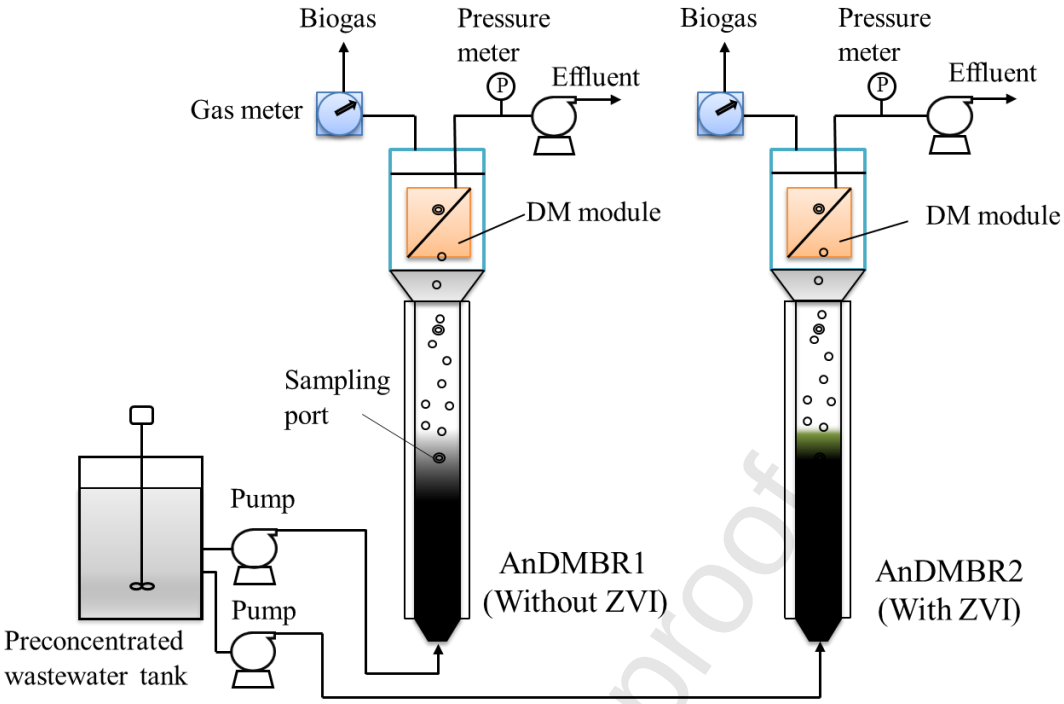

Fig. 1.

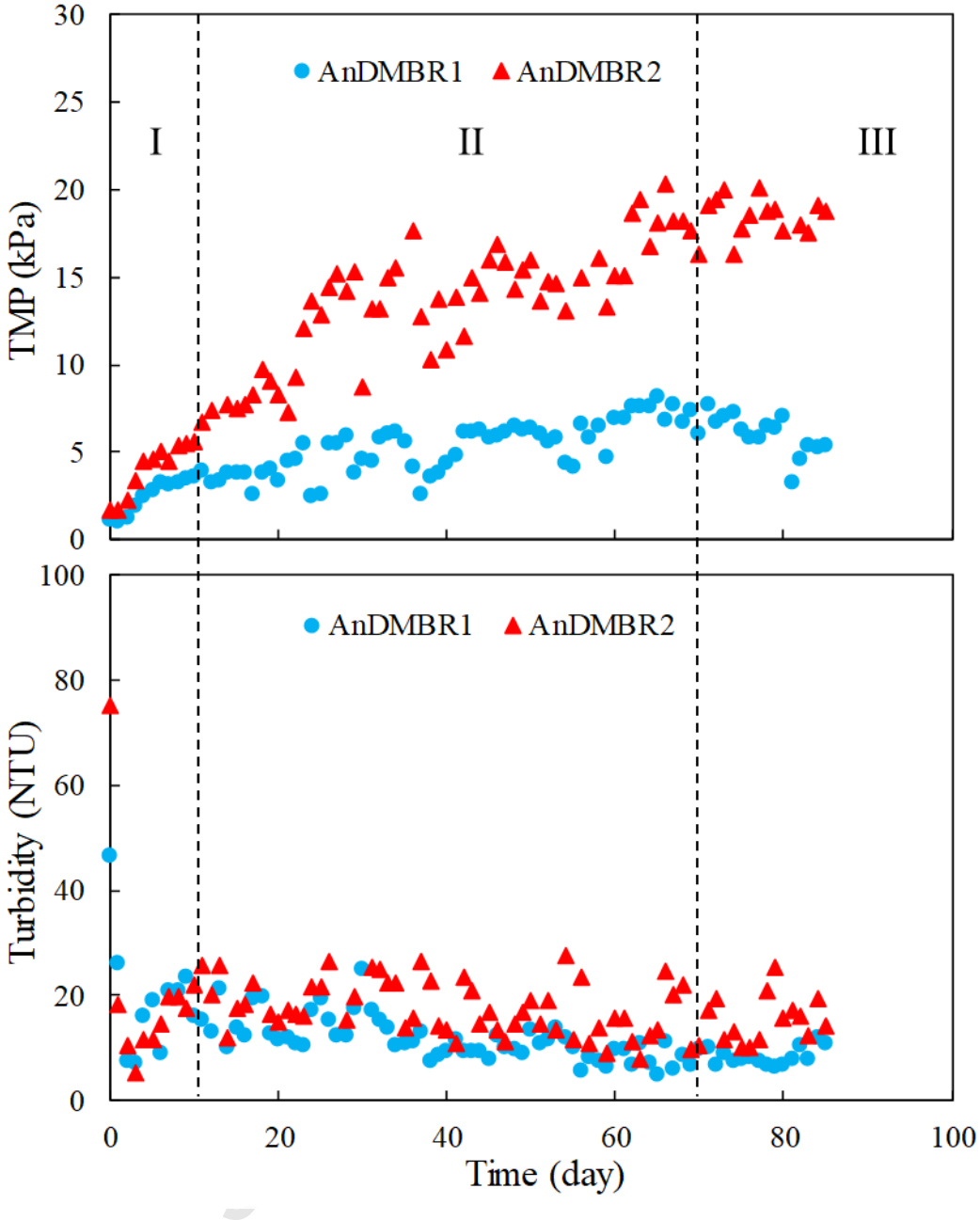
AnDMBR1
AnDMBR2
I
II
III
TMP (kPa)
Turbidity (NTU)
Time (day)
0
5
10
15
20
25
30
40
60
80
100
0
20
40
60
80
100

Fig. 2.

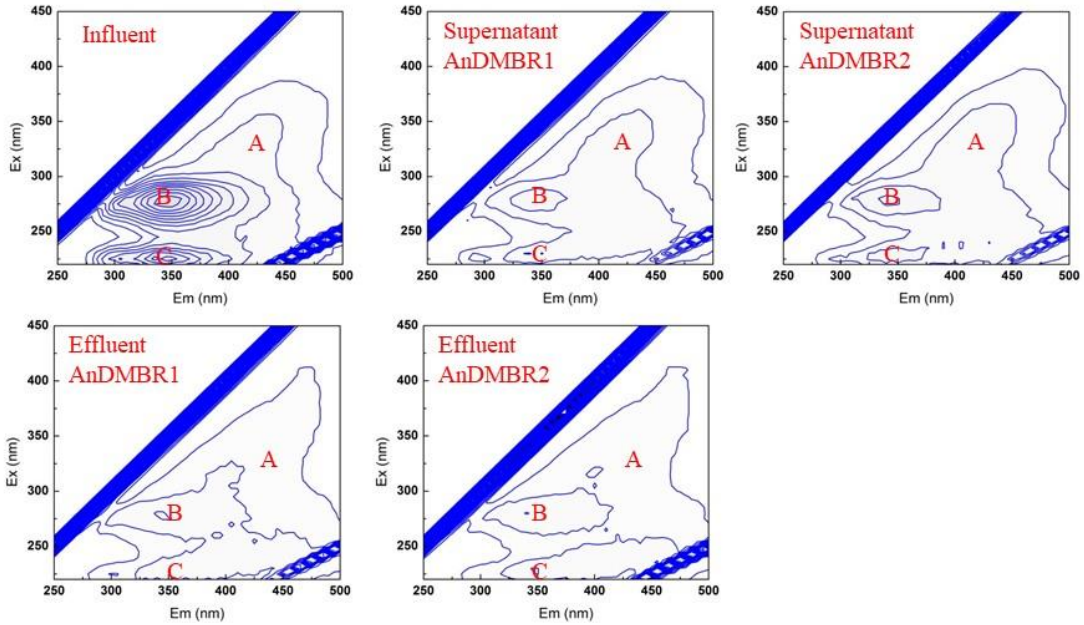

Fig. 3.

(a)

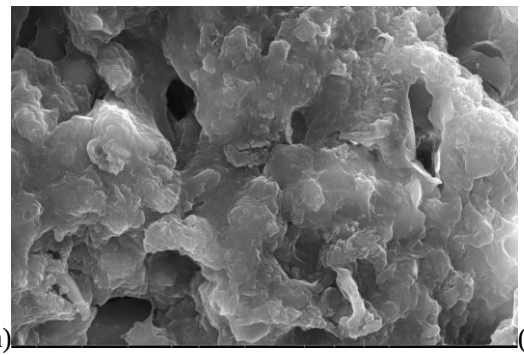

(b)

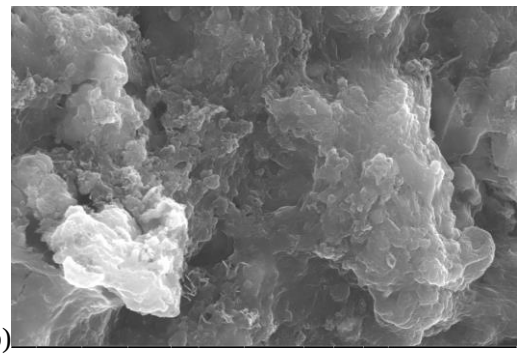

(c)

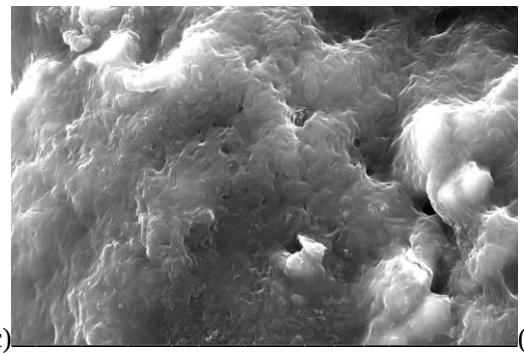

(d)

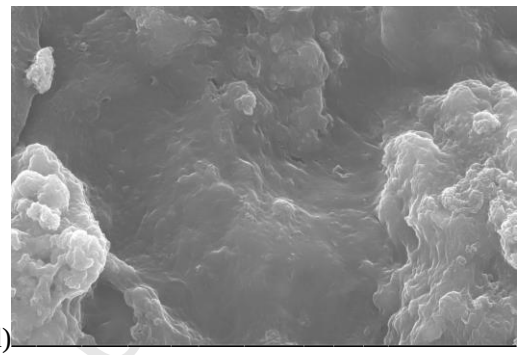

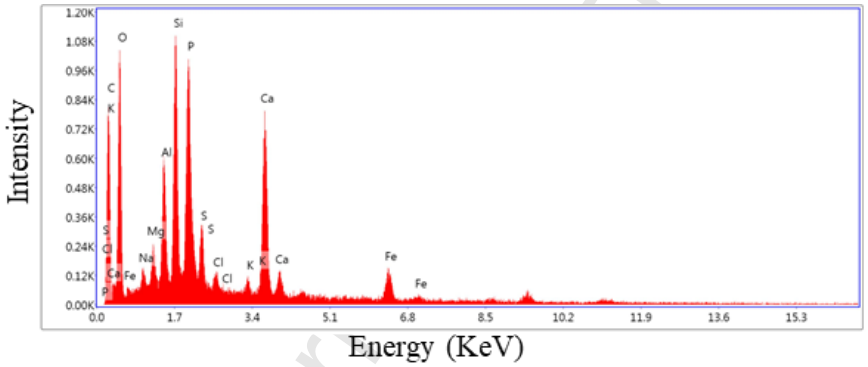
Intensity
Energy (KeV)
O
Si
P
C
K
Ca
Al
Mg
Na
Fe
S
Cl

(e)

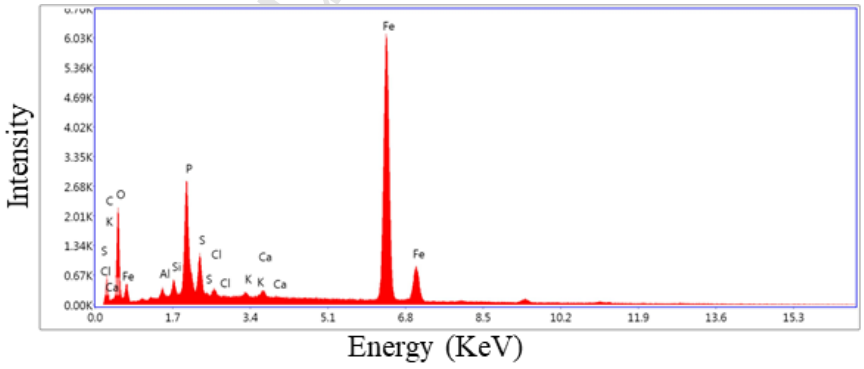
Intensity
Energy (KeV)
Fe
P
C
O
K
S
Cl
Ca
Al
Si

(f)

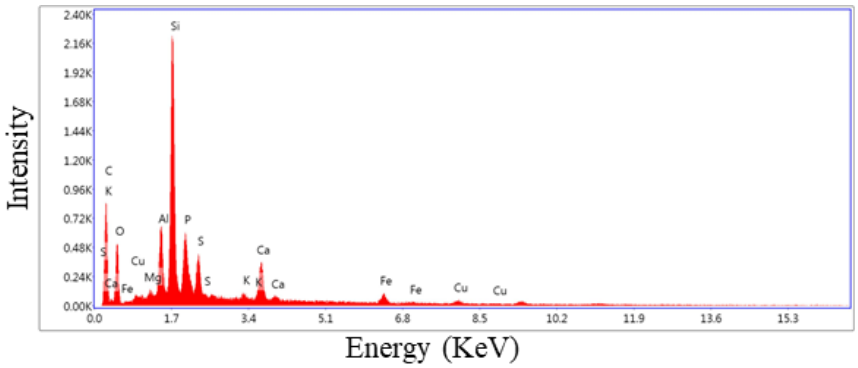

(g)

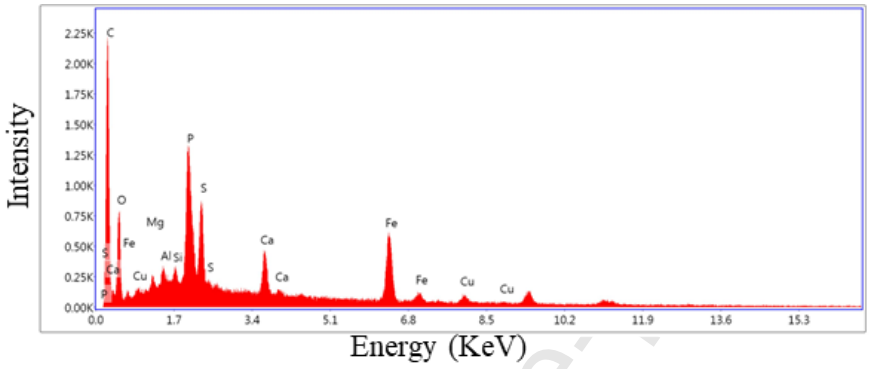

(h)

Fig. 4.

(a)

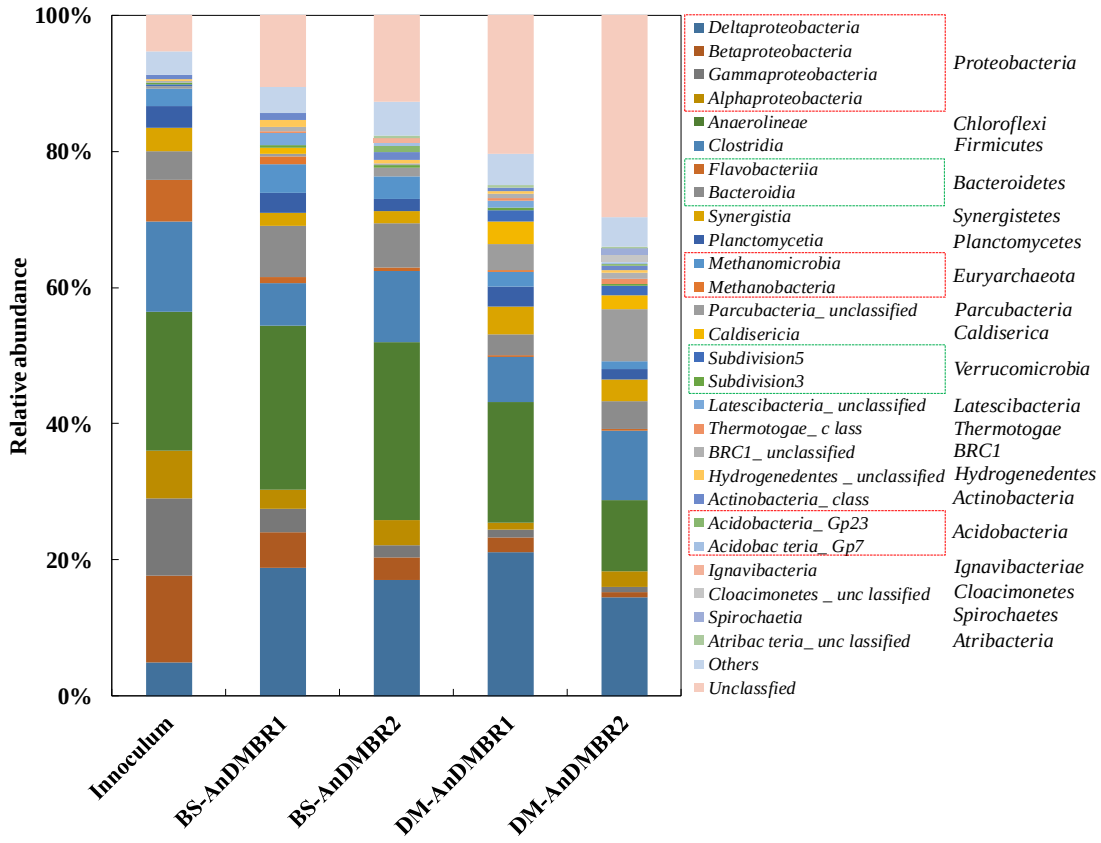

(b)

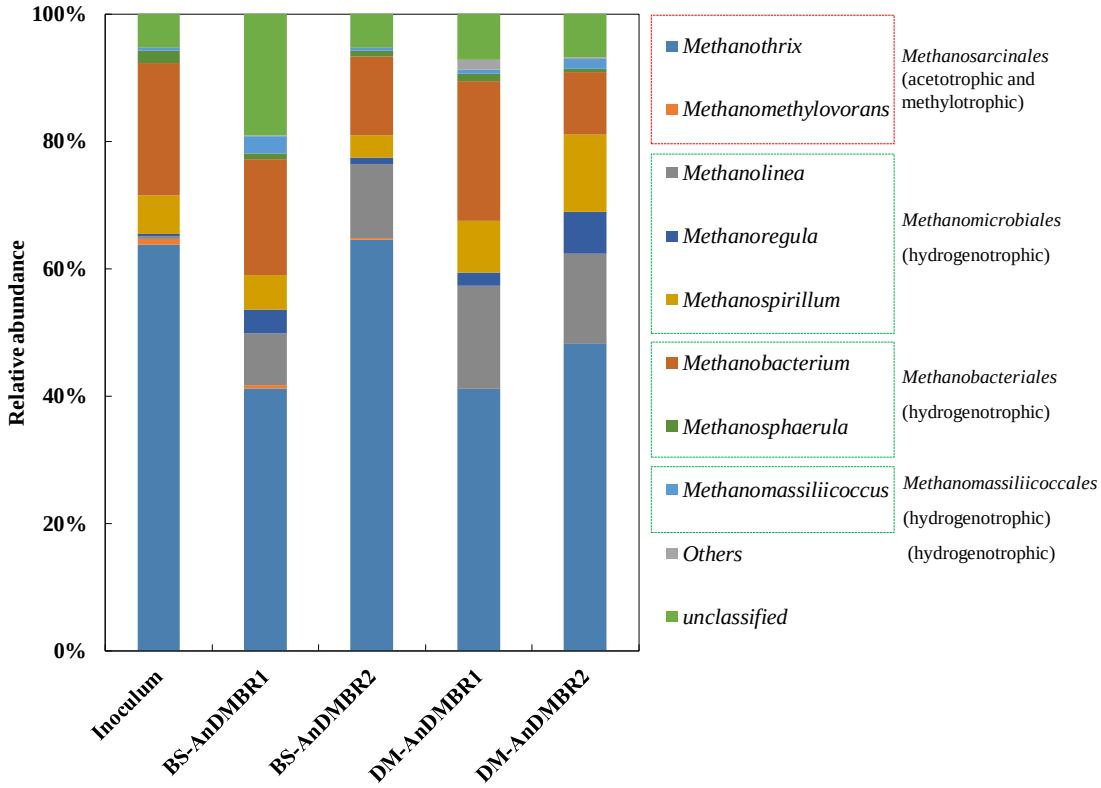

Fig. 5.

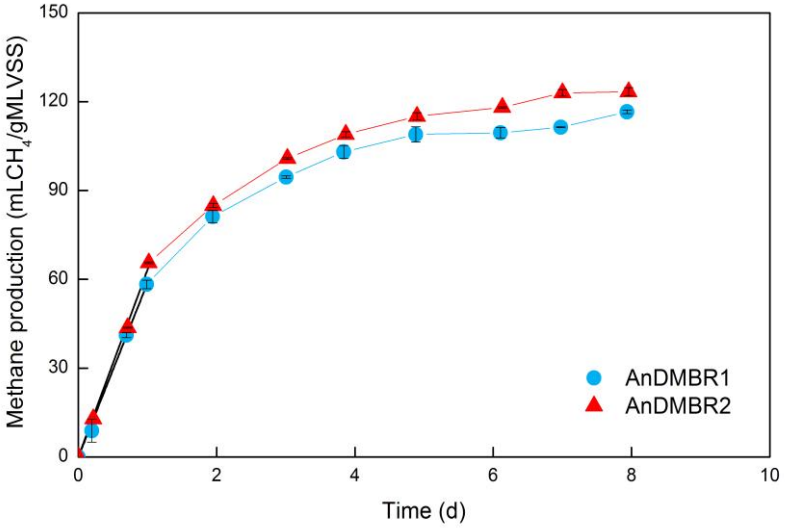
Methane production (mLCH4/gMLVSS)
Time (d)
AnDMBR1
AnDMBR2

(a)

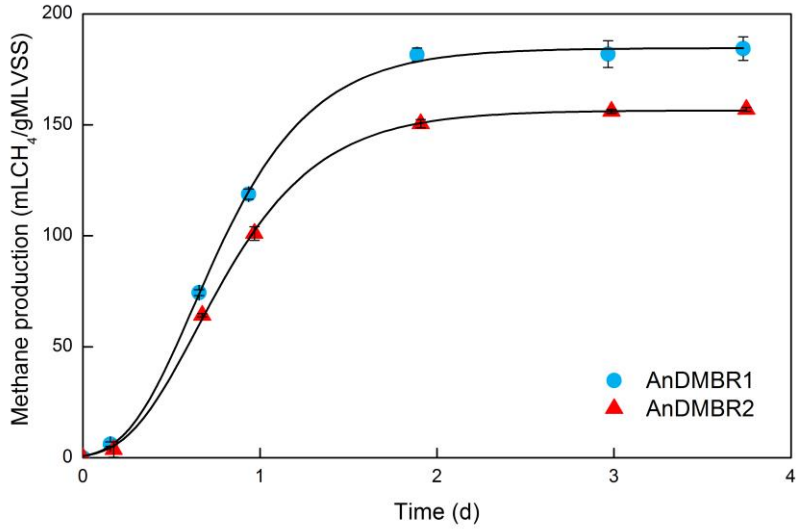
Methane production (mLCH4/gMLVSS)
Time (d)
AnDMBR1
AnDMBR2

(b)

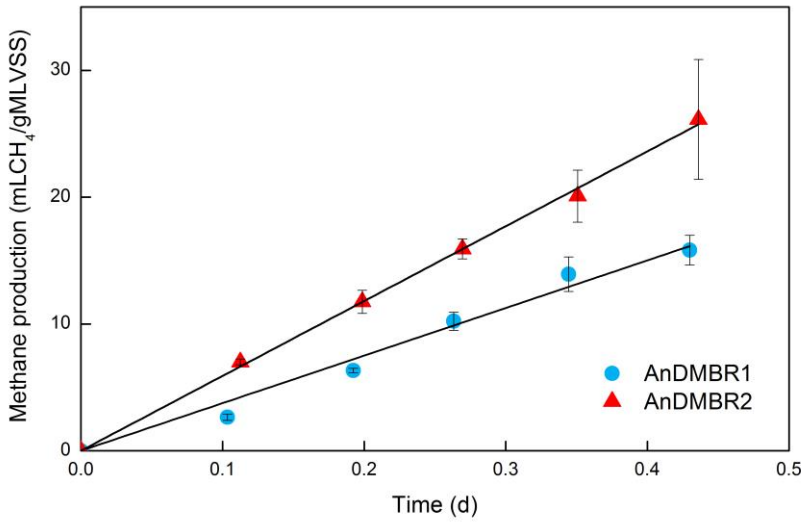
Methane production (mLCH4/gMLVSS)
Time (d)
AnDMBR1
AnDMBR2

(c)

Fig. 6.